molecular pharmaceutics

Article

pubs.acs.org/molecularpharmaceutics

Biological Characterization of Folate-Decorated Biodegradable Polymer–Platinum(II) Complex Micelles

Rui Wang,[†,‡] Xiuli Hu,[*,†] Sai Wu,[§] Haihua Xiao,[†,‡] Haidong Cai,[∥] Zhigang Xie,[†] Yubin Huang,[†] and Xiabin Jing[†]

[†]State Key Laboratory of Polymer Physics and Chemistry, Changchun Institute of Applied Chemistry, Chinese Academy of Sciences, Changchun 130022, People's Republic of China

[‡]Graduate School of Chinese Academy of Sciences, Beijing 100049, People's Republic of China

[§]Department of Material Science and Engineering, Jilin University, Changchun 130022, People's Republic of China

[∥]Department of Chemistry and Environmental Engineering, Changchun University of Science and Technology, Changchun 130022, People's Republic of China

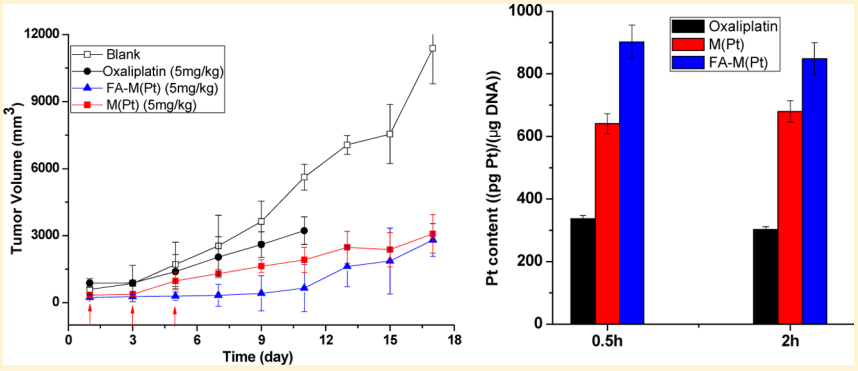

ABSTRACT: A biodegradable and amphiphilic copolymer, poly(ethylene glycol)-*block*-poly(L-lactide-*co*-2-methyl-2-carboxyl-propylene carbonate) (mPEG-*b*-P(LA-*co*-MCC)), which contains pendant carboxyl groups, was chosen as a drug carrier for the active anticancer part (diaminocyclohexane platinum, DACH-Pt) of oxaliplatin to form mPEG-*b*-P(LA-*co*-MCC/Pt) complex. A folic acid-conjugated copolymer, folic acid–poly(ethylene glycol)-*block*-poly(L-lactide) (FA–PEG-PLA), with similar chemical structure was chosen for targeting. Multifunctional micelles were successfully prepared by a coassembling method. In vitro evaluation was performed by using SKOV-3 and MCF-7 cancer cells. In vivo blood clearance of platinum was studied, and the results show that micelles exhibit longer blood circulation after iv injection. Pt biodistribution was studied by measuring its levels in plasma, organs, and tumors, especially in tumor cell DNA, by atomic absorption and inductively coupled plasma mass spectrometry. Antitumor activity was assessed in mice bearing H22 liver cancers, and the results showed that the micelles with FA moieties exhibited greater antitumor efficacy than those without FA or oxaliplatin. Therefore, these novel multifunctional platinum micelles have great potential in future clinical application.

KEYWORDS: *folic acid targeting, biodegradable, multifunctional micelles, polymer–platinum complex, oxaliplatin*

INTRODUCTION

Cisplatin, carboplatin, oxaliplatin and other platinum(II)-based drugs are widely employed in cancer chemotherapy and have greatly improved the prognosis for ovarian, lung and especially testicular cancer.[1−3] Among them, oxaliplatin, oxalato(*trans*-1,2-diaminocyclohexane)platinum(II), is the third generation of Pt anticancer compounds approved as first-line chemotherapy drug in combination with 5-fluorouracil for the treatment of advanced colorectal cancers worldwide.[4] Compared with cisplatin or carboplatin, oxaliplatin displays a better tolerability but still has side effects (acute dysesthesias, cumulative peripheral distal neurotoxicity) which limit its range of usable doses.[5,6]

In recent years, enormous effort has been dedicated to develop polymeric Pt complexes.[7,8] They are expected to overcome the side effects by prolonging the systematic circulation and to target the drugs to tumor sites via passive and active targeting. For polymeric Pt(II) complexes, the most investigated is cisplatin and the active anticancer part (DACH-Pt) of oxaliplatin. The used polymer carriers include chitosan,[9] dendrimers,[10] *N*-(2-hydroxypropyl) methacrylamide (HPMA) copolymers[11] and polyaspartamide[12]or polyglutamide[13]poly-

Received: May 24, 2012
Revised: August 17, 2012
Accepted: September 6, 2012
Published: September 6, 2012

polymers. However, most of these carrier polymers are water-soluble and nonbiodegradable. A promising carrier for platinum drugs is polymeric micelles. Polymeric micelles, self-assembled block copolymers with a core−shell structure, have several useful functions that benefit the protection and targeted delivery of platinum drugs.[14,15] They usually enter the cancer cells via endocytosis with considerable efficiency. The carrier polymer can be degraded and the encapsulated drugs can be released rapidly under the endosome or secondary lysosome conditions. The first generation of platinum-drug-loaded micelles was reported by Kataoka and his co-workers and was prepared by the metal-complex formation between *cis*-dichlorodiamineplatinum(II) (cisplatin, CDDP) or DACH-Pt and poly(ethylene glycol)-*b*-poly(amino acid) block copolymers.[13] Drug micelles showed remarkably prolonged blood circulation and greater accumulation in tumor tissue compared to free oxaliplatin.

Folic acid (FA) receptors are overexpressed in several human tumors including ovarian and breast cancers and rarely expressed in normal tissues, therefore, folic acid has been chosen as the targeting moiety and investigated in various drug carriers.[16,17] However, platinum-loaded micelles with folic acid as active targeting have not been reported. Herein, multifunctional micelles with targeting moieties and anticancer drugs were prepared by coassembling poly(ethylene glycol)-*block*-poly(L-lactide-*co*-2-methyl-2-carboxyl-propylene carbonate/platinum) (mPEG-*b*-P(LA-*co*-MCC/Pt)) complex and folic acid-poly(ethylene glycol)-*block*-poly(L-lactide) (FA-PEG-PLA) copolymer. The micellar physicochemical characters such as particle size, size distribution and drug loading were characterized. The in vivo behavior such as blood clearance, biodistribution, antitumor activity, Pt levels in plasma, tumors and tumor DNA were measured using Kunming mice bearing H22 liver cancer.

EXPERIMENTAL SECTION

Materials. The block copolymers poly(ethylene glycol)-*block*-poly(L-lactide-*co*-2-methyl-2-carboxyl-propylene carbonate) (mPEG-*b*-P(LA-*co*-MCC)) and folic acid-poly(ethylene glycol)-*block*-poly(L-lactide) (FA-PEG-PLA) were synthesized in our laboratory as previously described.[14,17] The copolymers used in this paper had the following specifications: $mPEG_{5000}$-*b*-$P(LA_{1000}$-*co*-$MCC_{960})$ and NH_2-PEG_{5400}-*b*-PLA_{3000} measured by proton nuclear magnetic resonance (^1H NMR), where the subscripts are molecular weights of the corresponding blocks or repeating units. K_2PtCl_4 was purchased from Shandong Boyuan Pharmaceutical Co. Ltd., China. ((1*R*,2*R*)-1,2-Diaminecyclohexano)platinum(II) dichloride (DACH-Pt-Cl_2 for short) was synthesized as previously described.[18] All other chemicals were used as received.

Platinum Analysis. Inductively coupled plasma optical emission spectrometry (ICPOES, iCAP 6300, Thermoscientific, USA) was used to determine the total Pt drug loading content of polymer−Pt complex and in the samples obtained outside of the dialysis bags in drug release experiments. Inductively coupled plasma mass spectrometry (ICP-MS, Xseries II, Thermoscientific, USA) was used for quantitative determination of trace levels of Pt.

Dynamic Light Scattering (DLS). Size distribution of micelles was determined by dynamic light scattering with a vertically polarized He−Ne laser (DAWN EOS, Wyatt Technologies, USA). The scattering angle was fixed at 90°, and the measurement was carried out at a constant temperature of 25 °C. The sample solutions were diluted in filtered double distilled water prior to analysis.

Preparation of the mPEG-*b*-P(LA-*co*-MCC/Pt) Micelles (M(Pt)). The synthesis of the complex of mPEG-*b*-P(LA-*co*-MCC) with DACH-Pt was described in the literature.[14]

Multifunctional micelles with FA targeting moieties were prepared via a coassembling method. Briefly, 80 mg of mPEG-*b*-P(LA-*co*-MCC/Pt) and 20 mg of FA-PEG-*b*-PLA were dissolved in 5 mL of DMSO, and then 10 mL of Milli-Q water was added dropwise to the above solution in the dark. After all the water was added, the suspension was dialyzed against water for 24 h and then freeze-dried to give sponge-like micelles (abbreviated as FA-M(Pt) hereafter). Similarly the drug-loaded micelles M(Pt) were prepared from mPEG-*b*-P(LA-*co*-MCC/Pt) only.

Cell Lines and Cell Culture. MCF-7, SKOV-3 and H22 cell lines were purchased from the Institute of Biochemistry and Cell Biology, Chinese Academy of Sciences, Shanghai, China. SKOV-3 cells were grown in RPMI 1640 (Life Technologies) supplemented with 0.03% L-glutamine, 100 U/mL penicillin and 100 μg/mL streptomycin in 5% CO_2 at 37 °C. MCF-7 and H22 cells were grown in Dulbecco's modified Eagle's medium (DMEM, GIBCO) supplemented with 10% heat-inactivated fetal bovine serum (FBS, GIBCO), 100 U/mL penicillin and 100 μg/mL streptomycin (Sigma), and the culture medium was replaced once very day.

Cytotoxicity of the Pt Micelles. The cytotoxicity test was conducted to evaluate in vitro antitumor activity of the empty polymer micelles mPEG-*b*-P(LA-*co*-MCC) (M), drug loaded micelles M(Pt) and FA-M(Pt) by the (3-(4,5-dimethylthiazol-2-yl)-2,5-diphenyltetrazolium bromide (MTT) assay. Briefly, MCF-7 and SKOV-3 cells harvested in a logarithmic growth phase were seeded in 96-well plates at a density of 10^5 cells per well and incubated in RPMI 1640 for 24 h. The medium was then replaced by empty micelles M, oxaliplatin, M(Pt) and FA-M(Pt) micelles at a final equivalent Pt concentration from 0.04 to 25 μg/mL (diluted by culture medium). The amount of drug-free polymer mPEG-*b*-P(LA-*co*-MCC) micelle was equal to that in mPEG-*b*-P(LA-*co*-MCC/Pt) micelles. The incubation was continued for 48 h. Then, 20 μL of MTT solution in PBS with the concentration of 5 mg/mL was added and the plates were incubated for another 4 h at 37 °C, followed by removal of the culture medium containing MTT and addition of 150 μL of DMSO to each well to dissolve the formazan crystals formed. Finally, the plates were shaken for 10 min, and the absorbance of formazan product was measured at 492 nm by a microplate reader.

Cellular Uptake of the Pt Micelles. Cellular uptake by MCF-7 and SKOV-3 cells was examined by direct Pt measurements of the cells by ICP-MS.

MCF-7 and SKOV-3 cells were seeded in 6-well plates. These cells were then treated with oxaliplatin, M(Pt) and FA-M(Pt) micelles with the Pt concentration in the culture medium of 0.25 μM and subsequently incubated at 37 °C for 0.5 or 2 h. After washing with PBS three times, cells were lysed by cell lysis buffer. The Pt contents in the cell lysis solution were determined by ICP-MS. Cellular Pt levels were expresssed in ng of Pt/10^6 cells. In order to evaluate the Pt concentration in cellular DNA, SKOV-3 cells were selected and DNA was isolated by using DNA purification kit (Invitrogen, USA), and the DNA was digested with DNase I before analysis of Pt content by ICP-MS. Total Pt−DNA adducts were expressed as (pg of Pt)/(μg of DNA).

dx.doi.org/10.1021/mp3002914 | *Mol. Pharmaceutics* 2012, 9, 3200−3208

Scheme 1. Chemical Structures of mPEG-*b*-P(LA-*co*-MCC/Pt) (A) and FA-PEG-PLA (B) and Illustration of Folate Decorated Composite Micelles Prepared via a Coassembly Method (C)

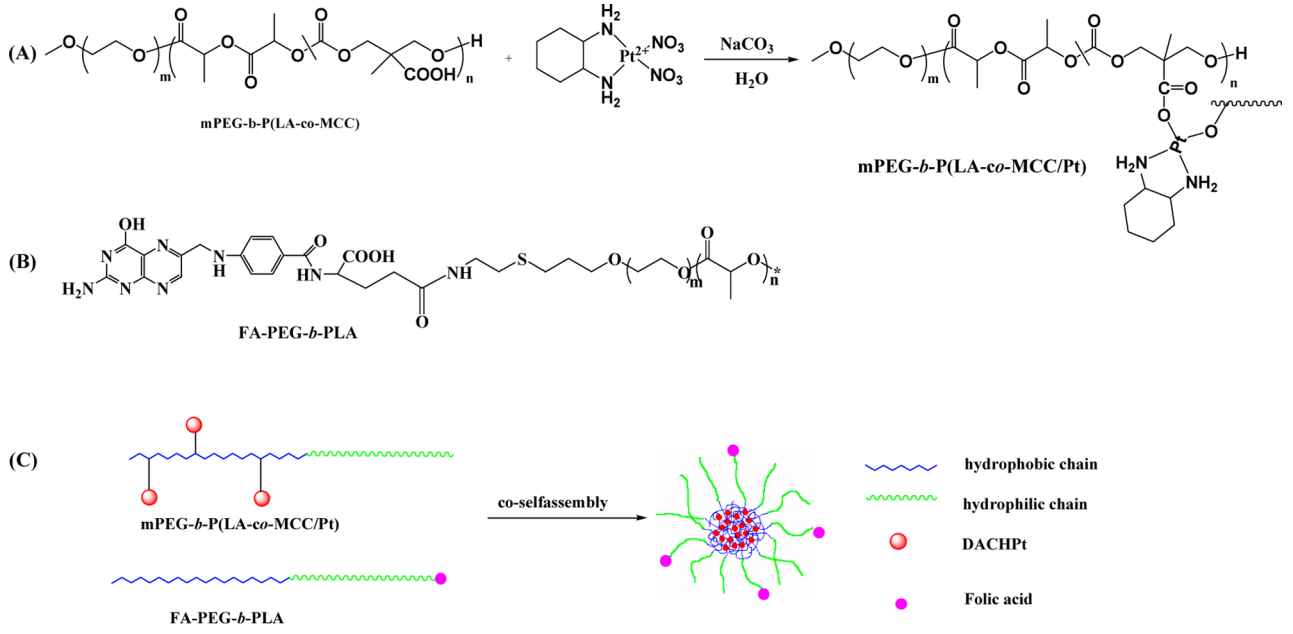

In Vivo Experiments. *Animals.* Kunming (KM) female mice were obtained from Jilin University, China (56−84 d, 20−25 g) and maintained under required conditions. Use of them for this study was approved by the Animal Ethics Committee of Jilin University. To develop the tumor xenografts, H22 cells were injected into the lateral aspect of the anterior limb of the mice (5×10^6 cells in 0.1 mL of PBS). After the tumor volume reached 50−200 mm^3, the hair of the mice was removed with a sodium sulfide solution (80 g/L in 30 vol % aqueous alcohol).

Blood Clearance. Twenty-four KM mice were randomly divided into four groups. The mice were injected with oxaliplatin, M(Pt) and FA-M(Pt) micelles via tail vein, respectively, with an equivalent Pt dose of 5 mg/kg body. Blood samples were collected into heparinized tubes right after injection (time point set as 5 s) and at time intervals (5 min, 15 min, 30 min, 1 h, 2 h, 6 h, 12 h) after administration. Subsequently, the blood samples were completely dissolved into 65% (v:v) nitric acid with heating and the platinum contents were measured by ICP-MS. In order to directly show the clearance of micelles from blood, the micelle quantity expressed as a percentage of the injected dose (% ID) was plotted as a function of time, assuming that the blood takes 7.2 wt % of the rat body weight. Using a nonlinear regression, the plasma data were fitted with a biexponential equation: $A(t) = A_1\ e^{-k_1 t} + A_2\ e^{-k_2 t}$, where $A(t)$ is the concentration of Pt in plasma and A_1, A_2, k_1 and k_2 are fitting parameters, from which pharmacokinetic parameters, such as plasma clearance rate (CL), steady-state area under the plasma concentration curve (AUC_{ss}) and mean residence time (MRT), could be calculated.

Biodistribution. Thirty-six KM mice were randomly divided into oxaliplatin, M(Pt) and FA-M(Pt) groups. The mice were injected with oxaliplatin, M(Pt) and FA-M(Pt) micelles via tail vein (3 mice each group), respectively (with an equivalent Pt dose of 5 mg/kg body) and then sacrificed at 2 h, 6 h, 12 h and 24 h. Major organs including liver, kidney and tumor were collected and washed with 0.9% saline before weighing. The organs were dissolved in 65% (v/v) nitric acid at 60 °C for 2 h, and Pt concentrations were measured by ICP-MS. In order to evaluate the Pt concentration in tumor DNA, the tumors at 24 and 48 h were selected and used to extract DNA, and the Pt concentration in DNA was determined by ICP-MS. Tumor DNA Pt levels were expressed as (pg of Pt)/(μg of DNA).

Antitumor Efficacy. Thirty-two mice bearing H22 tumor nodules were randomly divided into four groups: (1) normal saline (blank control), (2) oxaliplatin, (3) M(Pt) and (4) FA-M(Pt) groups. Before injection, all the mice were marked and weighed, and the length and width of the tumor were measured as the initial size on day 1. The day of starting injection was designated as day 1. For groups (2), (3) and (4), an equivalent Pt dose of 5 mg/kg body was intravenously injected via tail vein on day 1, day 3 and day 5, separately. For group (1), the mice were injected with an equivalent volume of normal saline. The tumor size was measured every other day, and the tumor volume (V) was calculated by the formula $V = (1/2)ab^2$, where a and b were the length and width of tumor, respectively. The mouse survival rate in each group was recorded daily.

RESULTS AND DISCUSSION

Preparation of FA-M(Pt). Recently, various kinds of multifunctional polymeric micelles have been exploited. Among the ways to form multifunctional micelles, coassembling of two or more amphiphilic block copolymers with different functions is a good choice because these copolymers can be synthesized separately without interference with each other, thus making the synthetic chemistry easy. In this paper, we constructed the composite micelles from two kinds of amphiphilic block copolymers, mPEG-*b*-P(LA-*co*-MCC/Pt) and FA-PEG-*b*-PLA. The two carrier polymers, $mPEG_{5000}$-*b*-$P(LA_{1000}$-*co*-$MCC_{960})$ and NH_2-PEG_{5400}-*b*-PLA_{3000}, measured by ^1H NMR, were synthesized in our own laboratory according to the reported procedures. The P(LA-*co*-MCC) stood for random copolymerization of L-lactide and trimethylene carbonate units with pendant carboxyl (COOH) groups. The diaminocyclohexane Pt (DACH-Pt), the active anticancer part of oxaliplatin, was selected and chelated with the pendant sodium carboxylates of mPEG-*b*-P(LA-*co*-MCC). Because one

dx.doi.org/10.1021/mp3002914 | *Mol. Pharmaceutics* 2012, 9, 3200−3208

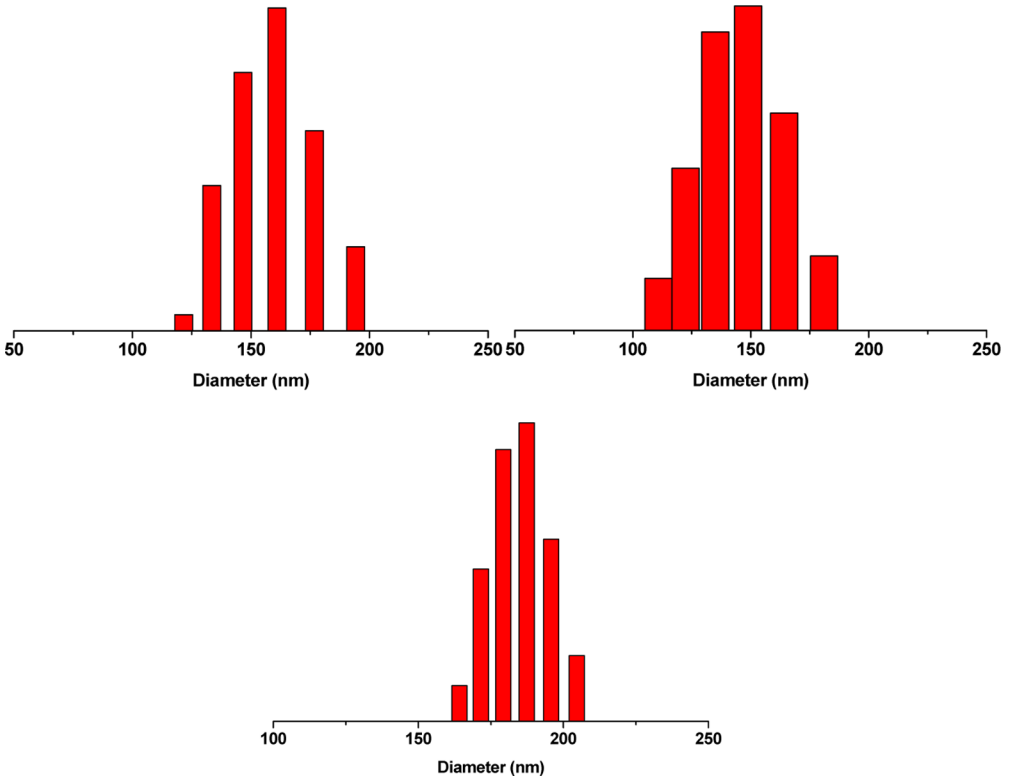

Figure 1. Size and size distribution of (A) mPEG-*b*-P(LA-*co*-MCC), (B) M(Pt) and (C) FA-M(Pt) micelles determined by DLS in water.

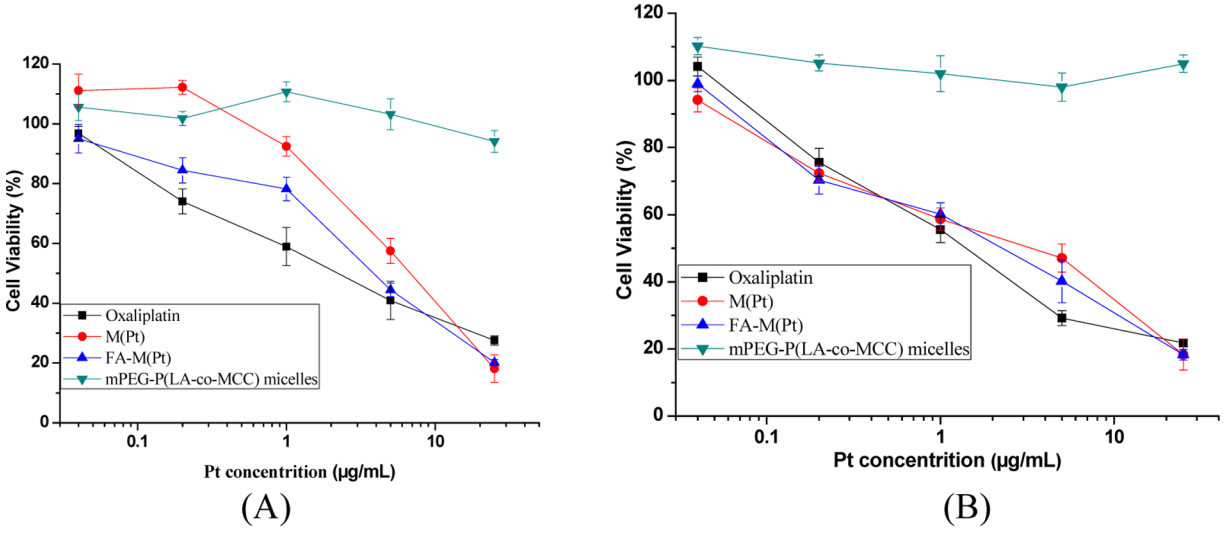

Figure 2. Cell viabilities of MCF-7 (A) and SKOV-3 cells (B) after 48 h incubation with empty micelles, oxaliplatin, M(Pt) and FA-M(Pt) micelles at various equivalent Pt concentrations (mean ± SD, n = 4).

Pt atom can chelate with two carboxyl groups, so the DACH-Pt chelated to the polymers in two ways: one DACH-Pt chelate with two carboxyl groups from a polymer chain or from different polymer chains. Unfortunately, we cannot distiguish the two forms. If the two carboxyl groups come from two different polymer chains, it is beneficial to stabilization of the micellar system.[14]

The Pt content in the complex was 12 wt % determined by ICP-OES. Folic acid-conjugated copolymer FA-PEG-*b*-PLA was selected for targeting. The chemical structure of mPEG-*b*-P(LA-*co*-MCC/Pt) (in short, M(Pt)) and FA-PEG-*b*-PLA are shown in Scheme 1, panels A and B, respectively. Due to their amphiphilic nature and similar block structures, mPEG-*b*-P(LA-*co*-MCC/Pt) and FA-PEG-*b*-PLA can coassemble in selective solvents. The hydrophobic P(LA-*co*-MCC/Pt) and PLA segments constitute the core of micelles, while the hydrophilic mPEG and FA-PEG segments form the shell of micelles as shown in Scheme 1. By using a coassembly method, "mixed micelles", which means every micelle was composed of FA-PEG-*b*-PLA and mPEG-*b*-P(LA-*co*-MCC/Pt) in a certain ratio, were obtained. A mixture of micelles means the two copolymers separately assemble into separate micelles. We have investigated similar coassembly micelles prepared by the same method using confocal laser scanning microscopy

dx.doi.org/10.1021/mp3002914 | *Mol. Pharmaceutics* 2012, 9, 3200−3208

(CLSM) in a previous paper[19] and found that the CLSM images were similar to those of bright field pictures, and there were no nonfluorescent micelles, which provided evidence for the coassembling of the two copolymers, not a mixture of micelles.

We assume that the two copolymers, mPEG-*b*-P(LA-*co*-MCC/Pt) and FA-PEG-PLA, are dispersed in the mixed micelles uniformly because of their similar segmental structures. Of course, there is a fluctuation in the FA number in each micelle and it is impossible to guarantee exactly the same amount and density of FA groups in each micelle. In order to obtain better targeting effect and higher drug loading content, the weight percent of FA-PEG-*b*-PLA in the composite micelles was selected to be 20 wt % and the obtained micelles were noted as FA-M(Pt). In a recently published paper,[20] the number of targeting moieties was calculated to be dozens to hundreds in each micelle. On one hand, the size of a targeting moiety is less than 1 nm. The micellar size and size distribution were detected by DLS, and Figure 1 gives the data. From Figure 1, we can see that the micellar size was in the range of 100−200 nm, and after complexing with DACH, the micelles become a little smaller (150 nm for mPEG-*b*-P(LA-*co*-MCC) and 125 nm for M(Pt)). Cells are in micrometer order of magnitude. Once one or two targeting moieties bind to cell surface, the others on the same micelle will not take effect because they cannot contact the cell surface due to the stereoposition in the space. Therefore, existence of these unbound targeting moieties does not influence the uptake of micelles.

In Vitro Cytotoxicity Assay. To examine the cytotoxicity of oxaliplatin, M(Pt), and FA-M(Pt) micelles, MCF-7 and SKOV-3 cells were selected and exposed to them in five doses (0.04, 0.2, 1, 5, 25 μg/mL Pt) for 48 h. The polymer carrier mPEG-*b*-P(LA-*co*-MCC) was similarly examined to evaluate its safety. Its amounts were equal to those in the corresponding mPEG-*b*-P(LA-*co*-MCC/Pt) micelle samples (Pt content: 12% w/w). The cytotoxicity was evaluated using MTT assay, and the results are presented in Figure 2. Very little toxicity to the two cell lines was observed for the copolymer carrier itself (Figure 2). As for the cytotoxicities of the three drug formulations, the following variation tendencies can be outlined from Figure 2. (1) Oxaliplatin, M(Pt) and FA-M(Pt) all showed a dose-dependent cytotoxicity toward the two cancer cell lines examined: higher dose of Pt drugs induces greater cell inhibition. (2) Different cancer cell lines display different responses to Pt drugs: (i) M(Pt) and FA-M(Pt) micelles exhibit lower cytotoxicity against MCF-7 than oxaliplatin itself; (ii) FA-M(Pt) micelles exhibit higher cytotoxicity against MCF-7 cancer cells than M(Pt); (iii) M(Pt) and FA-M(Pt) micelles exhibit similar cytotoxicity against SKOV-3 cancer cells as oxaliplatin. The IC_{50} values obtained from Figure 2 are listed in Table 1.

Cellular Uptake. Cellular uptake of oxaliplatin, M(Pt) and FA-M(Pt) by MCF-7 and SKOV-3 cells was assessed by directly measuring the Pt content in the cells by ICP-MS. The Pt content was expressed as "ng of Pt per 10^6 cells". As shown in Figure 3, when the cells were incubated for 0.5 h with oxaliplatin, M(Pt) and FA-M(Pt) at an equivalent initial Pt concentration of 0.25 μM, the Pt contents in the cells were 616.4, 487.8 and 745.4 ng of Pt/(10^6 cells) for MCF-7 cells and 1148.6, 1057.6, 1338.4 ng of Pt/(10^6 cells) for SKOV-3 cells, respectively. The Pt contents in the cells were 1671.2, 1257.6 and 1266.8 ng of Pt/(10^6 cells) for MCF-7 cells and 1358.0, 1332.4 and 2430.0 ng of Pt/(10^6 cells) for SKOV-3 cells incubated for 2 h, respectively. These data implied that oxaliplatin got internalized in the cells at a higher efficiency than M(Pt) and FA-M(Pt) micelles for MCF-7 cells, in agreement with higher cytotoxicity of oxaliplatin than M(Pt) and FA-M(Pt) micelles against MCF-7 cancer cells shown in Figure 2A. This is also supported by the result for free Dox and Dox micelles[21] that free drugs enter into cells by diffusion and micelles enter into cells by endocytosis. For SKOV-3 cells, there were similar Pt concentrations for oxaliplatin, M(Pt) and FA-M(Pt) micelles at 0.5 h and FA-M(Pt) micelles had higher Pt concentration at 2 h than oxaliplatin and M(Pt), in accordance with the higher cellular cytotoxicity of FA-M(Pt).

We also quantified the levels of bioavailable Pt in the internalized micelles and free oxaliplatin. We incubated SKOV-3 cells with free oxaliplatin, M(Pt) and FA-M(Pt) micelles for 0.5 and 2 h, followed by collecting and purifying the total DNA of the treated cells and measuring the Pt concentration in DNA using ICP-MS. As shown in Figure 4, the Pt content in the DNA from the SKOV-3 cancer cells was in the order oxaliplatin < M(Pt) < FA-M(Pt) for both 0.5 and 2 h. It is well-known that platinum(II) drugs cause apoptosis of cancer cells via chelating with the DNA strands to form Pt−DNA adducts. Therefore, the Pt content in the DNA sample would be a measure of the amount of platinum that is really responsible for cell death, or in short, therapeutically effective amount of platinum. Therefore, the data in Figure 4 convincingly support the effectiveness order of FA-M(Pt) > M(Pt) > oxaliplatin.

Plasma Pharmacokinetics. The concentration of total plasma Pt was determined as a function of time following single injection of oxaliplatin, M(Pt) and FA-M(Pt) micelles (equivalent Pt content of 5 (mg of Pt)/(kg body)) to mice bearing H22 liver cancer. As shown in Figure 5, the plasma platinum content after injection of oxaliplatin, M(Pt) or FA-M(Pt) decayed in a biexponential manner. By fitting the data with a biexponential equation ($A(t) = A_1\ e^{-k_1 t} + A_2\ e^{-k_2 t}$), pharmacokinetic parameters, such as plasma clearance rate (CL), steady-state area under the plasma concentration curve (AUC_{ss}) and mean residence time (MRT), were obtained (Table 2). From Figure 5 and these data, different blood circulation behaviors of the three groups were outlined as follows: (1) the plasma clearance of micelles was much slower than free oxaliplatin, as evidenced by the much greater AUC, slower CL and longer MRT; (2) the two curves of M(Pt) and FA-M(Pt) crossed each other at ca. 4 h, i.e., M(Pt) had higher plasma Pt concentration within 4 h, while FA-M(Pt) had higher plasma concentration after 4 h; (3) compared to M(Pt), FA-M(Pt) displayed a bigger AUC, slower CL and the same MRT, i.e., FA-M(Pt) was not as good as M(Pt) as far as the plasma drug concentration was concerned. This was probably due to the enhanced interaction between the FA moieties on the micelles and the blood proteins compared to the case of M(Pt) on which there were only biologically inert poly(ethylene glycol) segments.

Table 1. IC_{50} Values of Oxaliplatin, M(Pt) and FA-M(Pt) against MCF-7 and SKOV-3 Cell Lines

	IC_{50} (μg/mL)		
cell lines	oxaliplatin	M(Pt)	FA-M(Pt)
MCF-7	2.2	6.9	3.9
SKOV-3	1.4	3.2	2.3

dx.doi.org/10.1021/mp3002914 | *Mol. Pharmaceutics* 2012, 9, 3200−3208

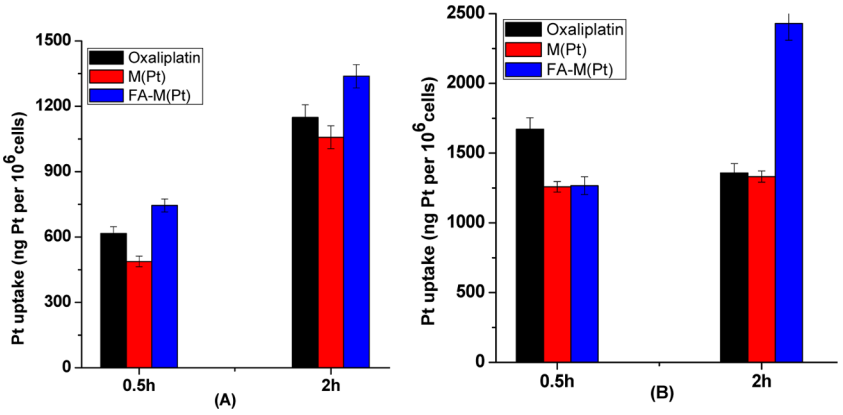

Figure 3. Pt uptake (ng of Pt per 10^6 cells) by MCF-7 and SKOV-3 cancer cells after 0.5 and 2 h incubation with oxaliplatin, M(Pt) and FA-M(Pt) micelles measured by ICP-MS (mean ± SD, n = 3).

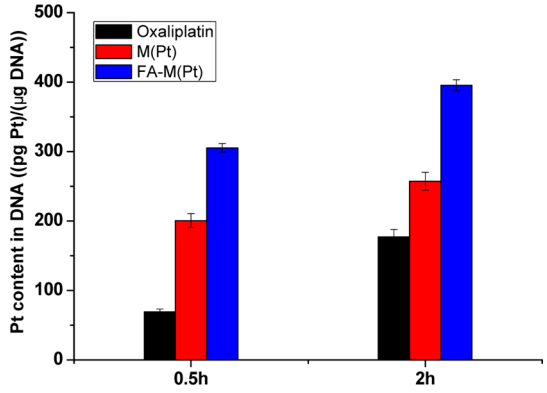

Figure 4. Pt content in the DNA collected from the SKOV-3 cancer cells treated with oxaliplatin, M(Pt) and FA-M(Pt) micelles for 0.5 and 2 h.

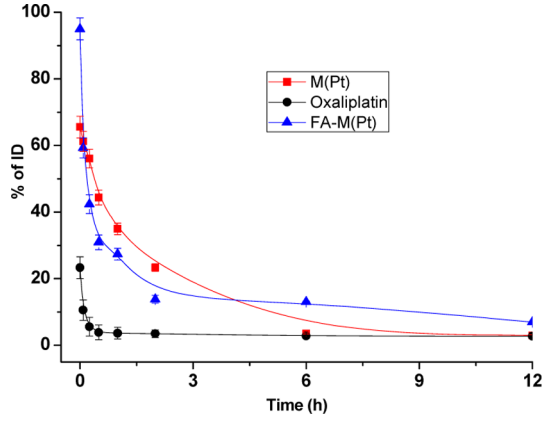

Figure 5. The blood clearance of free oxaliplatin, M(Pt) and FA-M(Pt) micelles.

Platinum Biodistribution in Organs and Tumor Tissues. To study the effects of the micelles on the biodistribution of Pt in vivo, we harvested the main viscera such as liver and kidney, and the tumor at different time points (2 h, 6 h, 12 h, 24 h) after the mice were injected intravenously with a single dose of free oxaliplatin and Pt micelles (Pt 5 mg/kg) and determined the Pt concentrations in the samples using ICP-MS. As shown in Figures 6A and 6B, significantly greater Pt accumulation was seen in liver and kidney for M(Pt) and FA-M(Pt) groups than that in the animals treated with free oxaliplatin, indicating that more micelles were taken up by the reticuloendothelial system (RES) in the liver than the free oxaliplatin, and most metabolized platinum species were excreted through kidneys. The higher population of FA-M(Pt) than M(Pt) after 12 h may have another reason, i.e., kidney cells themselves overexpress FA receptors. This may cause kidney damage, and further toxicity evaluation should be performed correspondingly to find out a balance between the targeting effect in tumor site and the possible damage in kidneys.

Table 2. Pharmacokinetic Parameters of Free Oxaliplatin, M(Pt) and FA-M(Pt) Micelles

parameter[a]	oxaliplatin	M(Pt)	FA-M(Pt)
A_1 (% ID)	19.9	49.5	64.6
A_2 (% ID)	4.0	16.5	30.4
K_1 (h^{-1})	12.8	0.4	7.9
K_2 (h^{-1})	0.04	2.28	0.16
$t^1_{1/2}$ (h) = 0.693/K_1	0.054	1.7	0.08
$t^2_{1/2}$ (h) = 0.693/K_2	16.7	0.3	4.2
AUC_{ss} (%ID·h)	97.7	132.6	192.1
CL (mL/h)	0.00009	0.00002	0.00001
MRT (h)	0.24	0.50	0.50

[a]The parameters were calculated from Figure 3, where $C_0 = A_1 + A_2$; $K = C_0/AUC_{ss}$; CL = KV; $AUC_{ss} = A_1/K_1 + A_2/K_2$; CL = dose/AUC; MRT = $(A_1/K_1^2 + A_2/K_2^2)/AUC$.

Figure 6C shows the Pt concentration changes in the tumor tissue after iv injection of oxaliplation, M(Pt) and FA-M(Pt). The Pt concentration vs time curves of M(Pt) and FA-M(Pt) groups are above that of the oxaliplatin group. If the relative Pt concentration over 1 was considered as a sort of targeting effect, the targeting effect had been established by less than 2 h for M(Pt) and by ca. 3 h for FA-M(Pt). This was due to the enhanced permeation and retention (EPR) effect of the M(Pt) and FA-M(Pt) micelles. Furthermore, the Pt concentration vs time curves of M(Pt) and FA-M(Pt) groups showed an upward slope followed by a downward slope. The M(Pt) group and FA-M(Pt) group displayed their maximum Pt concentrations at 6 and 12 h after drug administration, respectively, and the maximum Pt concentrations were more than 4 times and 3 times, respectively, than that in the oxaliplatin group. After 10 h, the Pt concentration in tumor was in the order of FA-M(Pt) group > M(Pt) group > oxaliplatin group, indicating that the active targeting effect due to the FA moieties prevailed over the EPR effect due to the particle size after this moment.

dx.doi.org/10.1021/mp3002914 | Mol. Pharmaceutics 2012, 9, 3200−3208

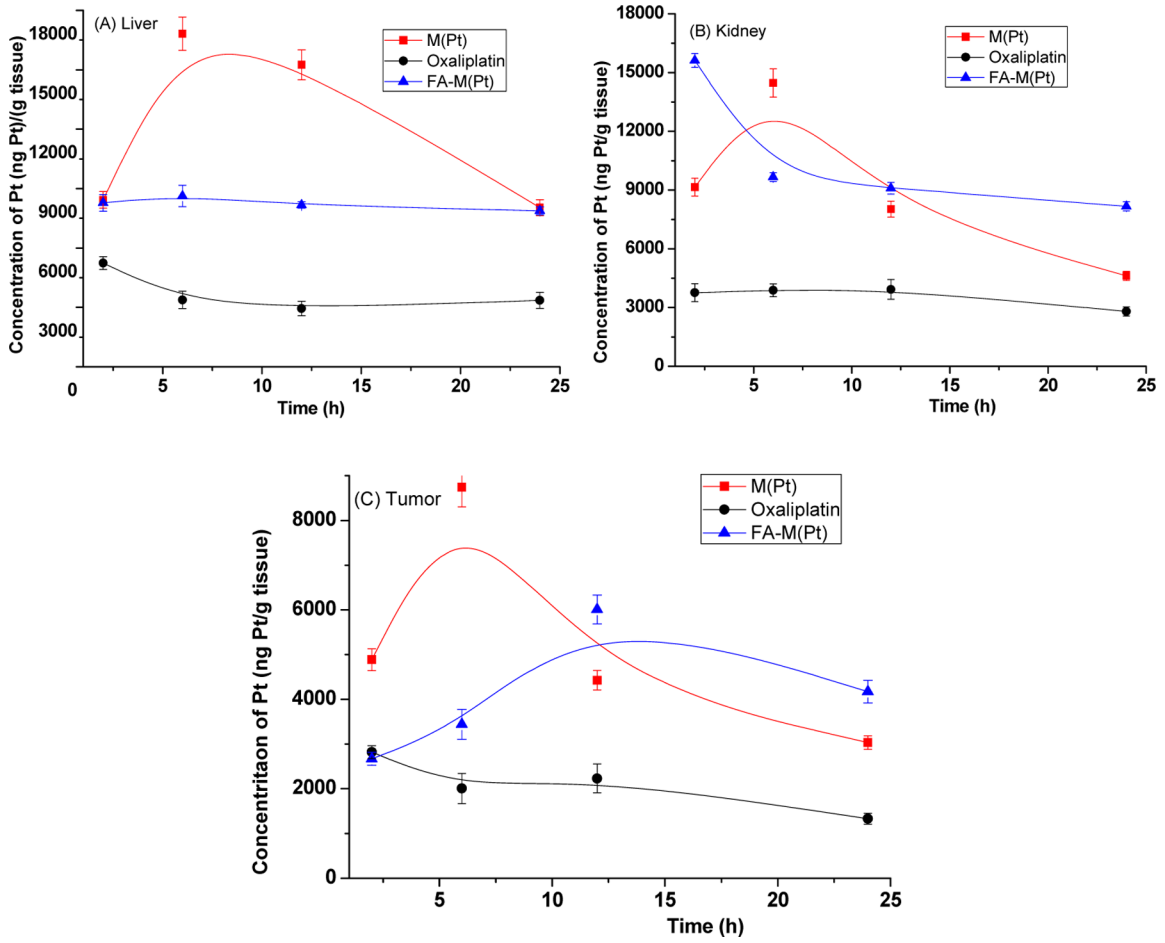

Figure 6. Biodistribution of Pt in mice treated with M(Pt), FA-M(Pt) micelles and free oxaliplatin in liver (A), kidney (B) and tumor (C) of the mice bearing H22 tumors at different time points after iv injection of a single dose (Pt 5 mg/kg).

Since only the activated Pt species can form Pt−DNA adducts, we collected and purified DNA from the tumor at 24 and 48 h after treatment and quantified the Pt level in the DNA sample. As shown in Figure 7, the Pt concentrations were significantly higher in DNA purified from mouse tumors treated with FA-M(Pt) micelles than those treated with M(Pt) micelles and free oxaliplatin. This marked increase in the Pt species of the Pt−DNA adducts probably explains the greater efficacy of FA-M(Pt) in anticancer discussed as follows.

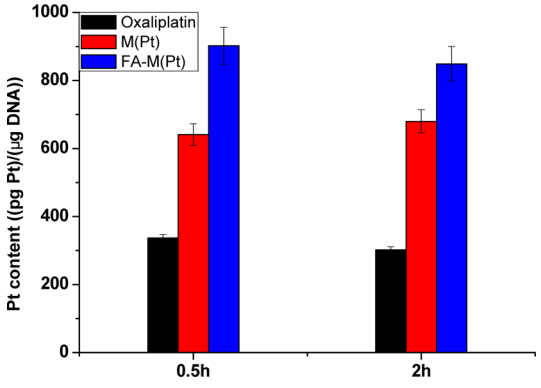

Figure 7. Pt content in the DNA separated from the H22-tumor-bearing KM mice injected with oxaliplatin, M(Pt) and FA-M(Pt) micelles.

In Vivo Antitumor Efficacy. To study the in vivo antitumor effect of FA-labeled and Pt-conjugated micelles, H22 xenograft models of hepatocarcinoma were established by injection of H22 cells into the lateral aspect of the anterior limb of KM mice. When the tumor grew to a size of 50−200 mm^3, 5 days after inoculation of the cancer cells, the mice were randomly divided into four groups with 8 mice in each group. The total equivalent dose of Pt (5 mg/kg) was given three times (on day 1, 3 and 5) via tail iv injection, and the tumor sizes were measured every other day. Figure 8 shows the tumor size as a function of time. It was notable that the administration of FA-M(Pt) was much more efficacious in tumor suppression compared with M(Pt) and free oxaliplatin. This was supported by the formation of more Pt−DNA adducts (Figure 7) in the cancer cells, and was consistent with the enhanced accumulation in the tumor bed (Figure 6C) and longer blood circulation for micelles (Figure 5) observed above. It is worth mentioning that, in ten days after drug administration, the oxaliplatin group mice all died and more than half were alive in the other three groups, indicating lower toxicity of the micelles. The survival curves are shown in Figure 8B.

■ CONCLUSIONS

In this paper we combined several concepts and techniques together, such as amphiphilic polymer carrier, polymer−drug conjugate, FA targeting, micelles etc., and successfully prepared multifunctional (targeting + antitumor) micelles from two

dx.doi.org/10.1021/mp3002914 | *Mol. Pharmaceutics* 2012, 9, 3200−3208

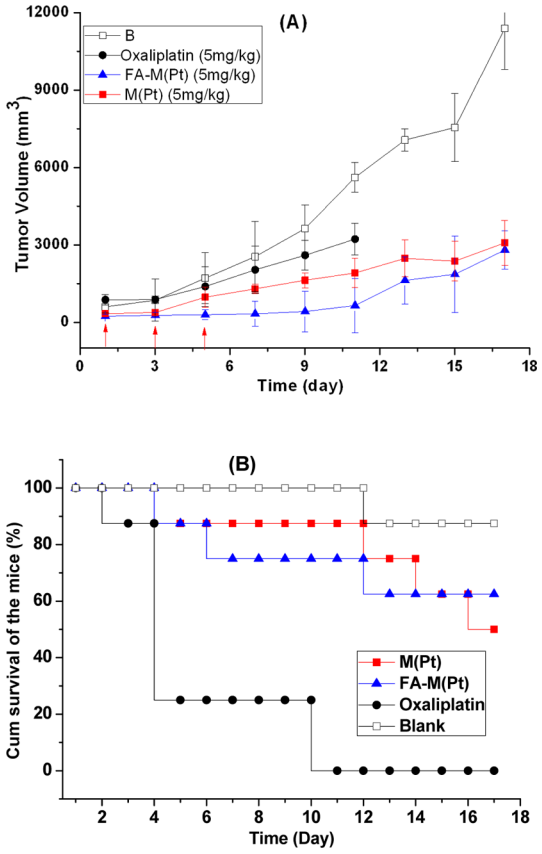

Figure 8. (A) Relative tumor sizes of mouse models bearing H22 liver cancers as a function of time after drug administration. The arrows represent the day on which the tail iv injection was performed. Bars indicate standard deviations. (B) Survival curves of mice bearing H22 liver cancers.

amphiphilic block copolymers: FA-PEG-*b*-PLA and mPEG-*b*-P(LA-*co*-MCC/Pt). The drug molecules were wrapped in the core part of the micelles, while FA resided in the corona of the micelles to effectively play a role of targeting moiety. In vitro and in vivo cytotoxicity and Pt biodistribution in plasma, organs and tumors, especially in tumor cell DNA, were measured. In vivo blood clearance showed that micelles exhibit longer blood circulation than free drug. Biodistribution studies showed that targeted micelles FA-M(Pt) led to increase in the Pt content in the tumor site, in tumor cells and in DNA of the tumor cells in comparison with the nontargeted M(Pt) micelles and free oxaliplatin, and consequently displayed a substantially better antitumor efficacy.

AUTHOR INFORMATION

Corresponding Author

*Changchun Institute of Applied Chemistry, Chinese Academy of Sciences, State Key Laboratory of Polymer Physics and Chemistry, Renmin street, 5625, Changchun 130022, People's Republic of China. Tel and fax: +86-431-85262779. E-mail: lily@ciac.jl.cn.

Notes

The authors declare no competing financial interest.

ACKNOWLEDGMENTS

Financial support was provided by the National Natural Science Foundation of China (Project No. 21004062, 51103148) and by the Ministry of Science and Technology of China ("973 Project", No. 2009CB930102).

REFERENCES

(1) Cicin, I.; Saip, P.; Eralp, Y.; Selam, M.; Topuz, S.; Ozluk, Y.; Aydin, Y.; Topuz, E. Ovarian carcinosarcomas: Clinicopathological prognostic factors and evaluation of chemotherapy regimens con taining platinum. *Gynecol. Oncol.* **2008**, *208*, 136−140.

(2) Wheate, N. J.; Walker, S.; Craig, G. E.; Oun, R. The status of platinum anticancer drugs in the clinic and in clinical trials. *Dalton Trans.* **2010**, *39*, 8113−8127.

(3) Wang, D.; Lippard, S. J. Cellular processing of platinum anticancer drugs. *Nat. Rev. Drug Discovery* **2005**, *4*, 307−320.

(4) Ibrahim, A.; Hirschfeld, S.; Cohen, M. H.; Griebel, D. J.; Williams, G. A.; Pazdur, R. FDA drug approval summaries: oxaliplatin. *Oncologist* **2004**, *9*, 8−12.

(5) Extra, J. N.; Espie, M.; Calvo, F.; Ferme, C.; Mignot, L.; Marty, M. Phase I study of oxaliplatin in patients with advanced cancer. *Cancer Chemother. Pharmacol.* **1990**, *25*, 299−303.

(6) Xiao, H. H.; Qi, R. G.; Liu, S.; Hu, X. L.; Duan, T. C.; Zheng, Y. H.; Huang, Y. B.; Jing, X. B. Biodegradable polymer-cisplatin(IV) conjugate as a pro-drug of cisplatin(II). *Biomaterials* **2011**, *32*, 7732−7739.

(7) Tong, R.; Cheng, J. J. Anticancer polymeric nanomedicines. *Polym. Rev.* **2007**, *47*, 345−381.

(8) Huynh, V. T.; Quek, J. Y.; de Souza, P. L.; Stenzel, M. H. Block Copolymer Micelles with Pendant Bifunctional Chelator for Platinum Drugs: Effect of Spacer Length on the Viability of Tumor Cells. *Biomacromolecules* **2012**, *13*, 1010−1023.

(9) Wang, Y. M.; Sato, H.; Adachi, I.; Horikoshi, I. Optimization of the formulation design of chitosan microspheres containing cisplatin. *J. Pharm. Sci.* **1996**, *85*, 1204−1210.

(10) Tomalia, D. A.; Reyna, L. A.; Svenson, S. Dendrimers as multi-purpose nanodevices for oncology drug delivery and diagnostic imaging. *Biochem. Soc. Trans.* **2007**, *35*, 61−67.

(11) Lin, X.; Zhang, Q.; Rice, J. R.; Stewart, D. R.; Nowotnik, D. P.; Howell, S. B. Improved targeting of platinum chemotherapeutics: The antitumour activity of the HPMA copolymer platinum agent AP5280 in murine tumour models. *Eur. J. Cancer* **2004**, *40*, 291−297.

(12) Caldwell, G.; Neuse, E. W.; van Rensburg, C. E. J. Cytotoxicity of selected water-soluble polymer-cis-diaminedichloroplatinum(II) conjugates against the human HeLa cancer cell line. *J. Inorg. Organomet. Polym.* **1997**, *7*, 217−231.

(13) Cabral, H.; Nishiyama, N.; Kataoka, K. Optimization of (1,2-diamino-cyclohexane)platinum(II)-loaded polymeric micelles directed to improved tumor targeting and enhanced antitumor activity. *J. Controlled Release* **2007**, *121*, 146−155.

(14) Xiao, H. H.; Zhou, D. F.; Liu, S.; Zheng, Y. H.; Huang, Y. B.; Jing, X. B. A complex of cyclohexane-1,2-diaminoplatinum with an amphiphilic biodegradable polymer with pendant carboxyl groups. *Acta Biomater.* **2012**, *8*, 1859−1868.

(15) Cabral, H.; Matsumoto, Y.; Mizuno, K.; Chen, Q.; Murakami, M.; Kimura, M.; Terada, Y.; Kano, M. R.; Miyazono, K.; Uesaka, M.; Nishiyama, N.; Kataoka, K. Accumulation of sub-100 nm polymeric micelles in poorly permeable tumours depends on size. *Nat. Nanotechnol.* **2011**, *6*, 815−823.

(16) Zhou, Y.; Wang, H.; Wang, C. X.; Li, Y. S.; Lu, W. F.; Chen, S. F.; Luo, J. D.; Jiang, Y. N.; Chen, J. H. Receptor-Mediated, Tumor-Targeted Gene Delivery Using Folate- Terminated Polyrotaxanes. *Mol. Pharmaceutics* **2012**, *9*, 1067−1076.

(17) Hu, X. L.; Wang, R.; Yue, J.; Liu, S.; Xie, Z. G.; Jing, X. B. Targeting and anti-tumor effect of folic acid-labeled polymer−Doxorubicin conjugates with pH-sensitive hydrazone linker. *J. Mater. Chem.* **2012**, DOI: 10.1039/c2jm31130e.

(18) Vollano, J. F.; Al-Baker, S.; Dabrowiak, J. C.; Schurig, J. E. Comparative antitumor studies on platinum(II) and platinum(IV) complexes containing 1,2-diaminocyclohexane. *J. Med. Chem.* **1987**, *30*, 716−719.

(19) Ma, P. A.; Liu, S.; Huang, Y. B.; Chen, X. S.; Zhang, L. P.; Jing, X. B. Lactose mediated liver-targeting effect observed by ex vivo imaging technology. *Biomaterials* **2010**, *31*, 2646−2654.
(20) Yue, J.; Liu, S.; Wang, R.; Hu, X. L.; Xie, Z. G.; Huang, Y. B.; Jing, X. B. Transferrin-conjugated micelles: enhanced accumulation and antitumor effect for transferrin-receptor-overexpressing cancer models. *Mol. Pharmaceutics* **2012**, *9*, 1919−1931.
(21) Hu, X. L.; Liu, S.; Huang, Y. B.; Chen, X. S.; Jing, X. B. Biodegradable Block Copolymer-Doxorubicin Conjugates via Different Linkages: Preparation, Characterization, and In Vitro Evaluation. *Biomacromolecules* **2010**, *11*, 2094−2102.